


Article

Sulfur Dioxide and Sulfolane as Additives in Organic Electrolytes to Develop Room-Temperature Sodium Batteries

Débora Ruiz-Martínez ^{1,*} and Roberto Gómez ^{2,*} ¹ Departament de Química Física, Universitat d'Alacant, Apartat 99, E-03080 Alicante, Spain² Institut Universitari d'Electroquímica, Universitat d'Alacant, Apartat 99, E-03080 Alicante, Spain

* Correspondence: debora.rm@ua.es (D.R.-M.); roberto.gomez@ua.es (R.G.)

Abstract: Sodium metal anodes have attracted great attention for the development of a next generation of high-energy batteries because of their high theoretical capacity (1166 mAh·g⁻¹), low redox potential (−2.71 V vs. SHE), and abundance. However, sodium reacts with most of the liquid electrolytes described to date and it has the shortcoming of dendrite formation during sodium deposition. Several strategies have been proposed to overcome these issues, including the incorporation of electrolyte additives. This work reports on the use of SO₂ and sulfolane as additives in organic electrolytes to modify the sodium–electrolyte interphase, making the sodium plating/stripping process more robust. Not only is the process more stable in the case of sodium metal anodes, but also the use of copper substrates is enabled. In fact, high-quality sodium films on copper have been attained by adding small mole fractions of the additives, which paves the way for the development of anode-free batteries. In a general vein, this work stresses the importance of researching on compatible and cost-effective additives that can be easily implemented in practice.

Keywords: sodium metal batteries; electrolyte additives; sodium plating/stripping; organic electrolytes; sulfur dioxide; sulfolane



Citation: Ruiz-Martínez, D.; Gómez, R. Sulfur Dioxide and Sulfolane as Additives in Organic Electrolytes to Develop Room-Temperature Sodium Batteries. *Batteries* **2022**, *8*, 127. <https://doi.org/10.3390/batteries8090127>

Academic Editor: Seung-Tae Hong

Received: 30 June 2022

Accepted: 5 September 2022

Published: 14 September 2022

Publisher's Note: MDPI stays neutral with regard to jurisdictional claims in published maps and institutional affiliations.



Copyright: © 2022 by the authors. Licensee MDPI, Basel, Switzerland. This article is an open access article distributed under the terms and conditions of the Creative Commons Attribution (CC BY) license (<https://creativecommons.org/licenses/by/4.0/>).

1. Introduction

The development of energy storage systems is one of the main challenges in this century, directly connected to the implementation of renewable energy sources. Rechargeable batteries, which have experienced a remarkable evolution over the past years, show attractive features for this purpose. In this context, lithium-based batteries have been the most studied and commercialized, particularly for portable devices and electromobility. However, because of the rather localized geographical distribution of lithium, relative scarcity, and high environmental impact of lithium extraction, significant efforts have focused on the development of alternative alkaline metal batteries. In this respect, sodium metal shows excellent electrochemical properties such as high theoretical specific capacity (1165 mAh g⁻¹) and low redox potential (−2.71 V vs. SHE), having also high abundance, wide distribution, and ample availability.

Sodium metal batteries (SMB), such as the Na-S and Na-NiCl₂ (ZEBRA) batteries, have been commercialized for a long time [1–3], although in a non-generalized way because of safety issues derived from their high operation temperature (up to 300 °C). This is an important reason why the scientific community is making a great effort to develop room-temperature sodium batteries. Several advances have been reported in the last few years; however, one of the main difficulties continues to be the high reactivity of sodium metal with most of the electrolytes commonly employed [4]. Ideally, an effective solid electrolyte interface (SEI) would be formed at the sodium surface, favoring stability and, at least, mitigating the dendritic growth that sodium typically undergoes in room-temperature SMBs. In practice, many strategies have been proposed aiming to improve the performance of sodium metal anodes, for instance by tuning the electrolyte formulation for improving the sodium plating/stripping process.

One common methodology consists of including a certain concentration of an additive in the organic electrolyte formulation to modify the SEI composition [5–7]. The use of ionic liquids and highly concentrated electrolytes has also been proposed. Among all ionic liquids in the literature, those containing the fluorosulfonylimide FSI[−] anion are particularly relevant as they generate an SEI that hinders the reactivity of sodium metal [8–11]. On the other hand, highly concentrated electrolytes are less reactive, and the sodium dendritic growth is limited since there is no sodium depletion in the vicinity of the electrode [12]. For instance, Zang et al. reported on the use of 4 M NaFSI in THF and DME solutions for Na plating/stripping on copper, displaying excellent electrochemical properties [13]. However, these electrolytes typically present low specific conductivity and they are costly, even at the laboratory scale.

Another less common, but very promising strategy is the use of inorganic electrolytes. Kim et al. reported the sulfur dioxide solvate NaAlCl₄·2SO₂ as an inorganic electrolyte for SMBs [14,15]. This electrolyte has a concentration above 5 M sodium ions in SO₂ and a specific conductivity of 0.1 S cm^{−1}. Non-dendritic sodium deposition at room temperature was specifically demonstrated. Recently, we described the use of a few ammonia-based liquids as electrolytes [16], specifically NaI, NaBF₄, and NaBH₄ were used as sodium salts, which were dissolved in liquid ammonia to generate each electrolyte (ammonia solvate). These liquids show excellent physicochemical properties such as a high sodium concentration (over 7 M) and an ionic conductivity close to 100 mS cm^{−1}. In addition, the Coulombic efficiency for the sodium plating/stripping process was virtually 100% for several hundreds of charge-discharge cycles. The use of copper foil as a substrate for effective sodium plating/stripping in these electrolytes was also shown, paving the way for the development of anode-free (anodeless) batteries. Despite these impressive properties, liquid inorganic electrolytes generally show lower boiling points than typical organic ones, and the working potential window is also narrower in the case of the ammonia solvates.

In this work, we report for the first time on the use of SO₂-based compounds as additives for some organic electrolytes commonly used in the context of SMBs. In particular, we have studied the effect of low mole fractions of either liquid SO₂ or sulfolane in electrolytes such as NaCF₃SO₃ (NaTf) in DOL:DME, NaSCN in DOL:DME, and NaClO₄ in propylene carbonate (PC). With the addition of the SO₂-based compounds, there is a significant improvement of the sodium plating/stripping process, achieving Coulombic efficiencies above 90% as demonstrated by cyclic voltammetry. Dramatic and promising changes in the aspect of the sodium film deposited on a copper substrate have been observed in the presence of the additives.

2. Results and Discussion

This contribution aims to illustrate the role of SO₂ and sulfolane as additives for SMB electrolytes. For this research, we have tested the sodium plating/stripping process in three organic electrolytes, namely 2 M sodium triflate (NaTf), 2 M NaSCN in a mixture of 1/1 *v/v* anhydrous DOL:DME, and 1 M NaClO₄ in anhydrous propylene carbonate. In each case, several concentrations of SO₂ and sulfolane were studied, varying from 0.02 to 0.2 in mole fraction.

Figure 1 shows the effect of adding SO₂ to the electrolytes mentioned above on sodium metal deposition and stripping by means of cyclic voltammograms (CVs). In all cases, current varies linearly with applied potential as observed previously (linear polarization) [17]. Figure 1a,c,e shows ten successive CVs for the Na⁺/Na process without additive using ± 0.2 V as the potential window. There is a progressive and significant decrease of the current density as the cycle number increases, particularly in the case of the 2 M NaTf/DOL:DME electrolyte, for which the currents halve after 10 CVs. This behavior can be related to the formation of an SEI on the sodium surface, probably linked to the decomposition of the organic electrolyte. This process has been widely described in the literature by many authors [5,6]. In contrast, when a certain amount of additive is present in the electrolyte, the trend observed during cycling changes. In fact, the addition of SO₂ mole

fractions of 0.02 or 0.05 consistently leads to a stabilization of the sodium plating/stripping process, the voltammograms experiencing less changes upon repeated cycling. Further information about the evolution of the voltammetric response upon 10 cycles for each electrolyte and SO_2 concentration is provided in the Supplementary Materials (Figures S1–S3).

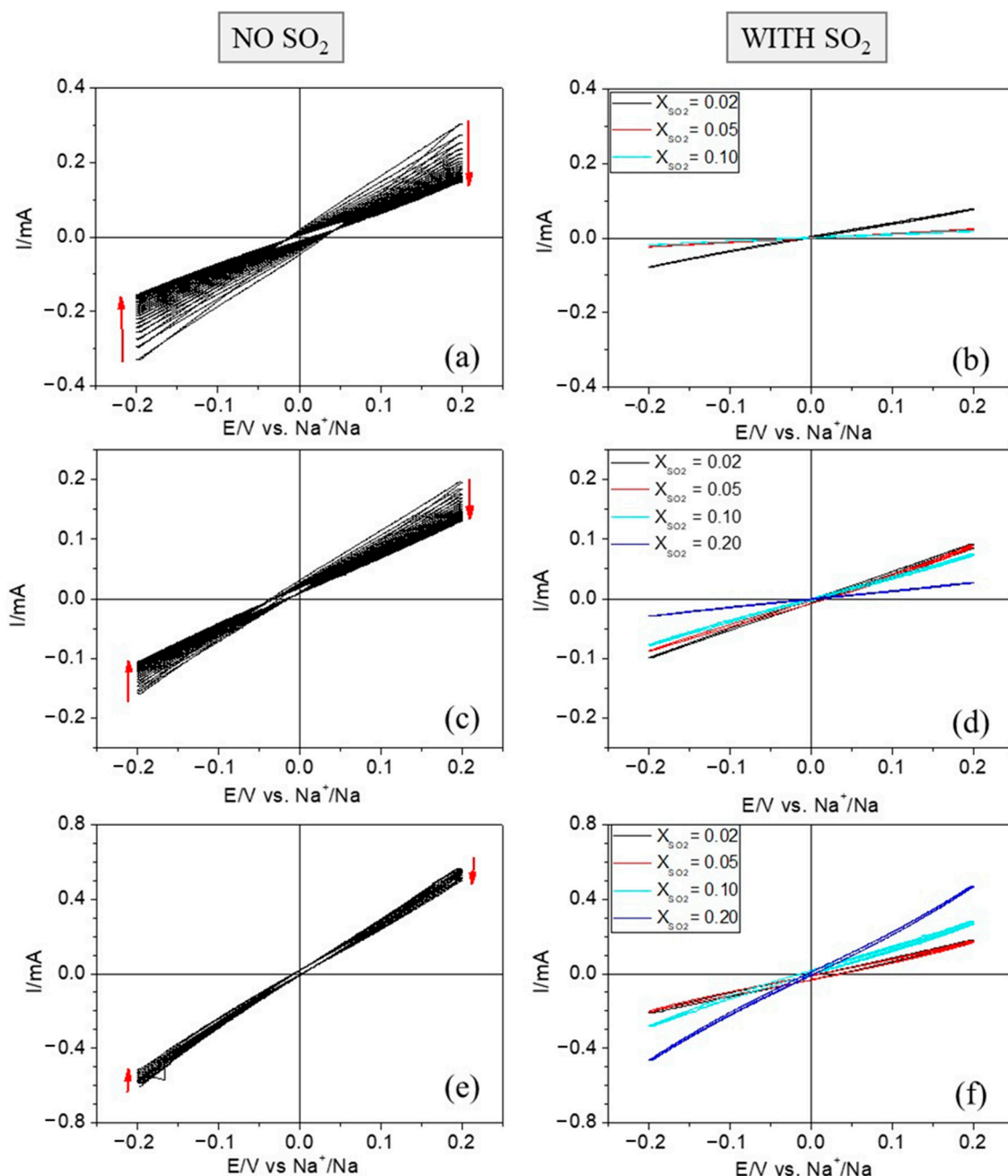


Figure 1. Cyclic voltammograms in the presence and the absence of SO_2 for Na electrodes in different organic electrolytes: (a) 2 M NaTf/DOL:DME, (b) 1.6 M NaTf/DOL:DME; (c,d) 2 M NaSCN/DOL:DME and (e,f) 1 M NaClO₄/PC at 20 mV s⁻¹.

On the other hand, colored curves in Figure 1b,d,f correspond to the tenth cycle for each SO_2 concentration and for each electrolyte. By comparing them with the CVs in the absence of additive, a decrease of the currents is generally observed. The ohmic behavior of the voltammograms allows us to describe them in terms of resistances. In a comprehensive work on lithium plating, based mainly on voltammetric measurements, Genovese et al. calculated the so-called plating resistance from the slope of the current–potential curve

from 0 to -300 mV vs. Li^+/Li , and they considered that tracking such a resistance was a good gauge of lithium cycling performance [18]. Analogously, we define here the plating-stripping resistance for the Na^+/Na process as:

$$R_{ps} = \left(\frac{\partial E}{\partial I} \right)_{I=0} \quad (1)$$

where E stands for the potential vs. Na^+/Na and I for the current, as well as its change over 10 voltammetric cycles (ΔR_{ps}). The plating-stripping resistance contains contributions from more fundamental magnitudes, including the liquid electrolyte resistance, the SEI resistance, and the charge transfer resistance. Changes in the magnitude of the plating resistance in the case of lithium were attributed to changes in the SEI composition [18]. Table 1 gathers the resistance values before the addition of sulfur dioxide, and it also shows the effect of the mole fraction of sulfur dioxide on R_{ps} . These values are in the same order of magnitude as those found for lithium deposition [18]. The addition of sulfur dioxide triggers two main effects: (i) an increase in the plating-stripping resistance values and (ii) a significant stabilization of the CVs.

Table 1. Plating-stripping resistance for sodium anodes in contact with three different electrolytes. Values for cycles 1 and 10 are given, together with the corresponding variation (ΔR_{ps}). Plating-stripping resistance (cycle 10) is also given upon the addition of different mole fractions of sulfur dioxide. * NaTf concentration was 1.6 M in the presence of SO_2 .

Electrolyte	$R_{ps}(\text{Cycle 1})/\text{k}\Omega$	$R_{ps}(\text{Cycle 10})/\text{k}\Omega$	$\Delta R_{ps}/\text{k}\Omega$	X_{SO_2}	$R_{ps}(\text{SO}_2)/\text{k}\Omega$
2 M NaTf/ DOL:DME *	0.62	1.28	0.66	0.02	2.48
				0.05	10
				0.10	10
2 M NaSCN/ DOL:DME	1.1	1.72	0.62	0.02	2.0
				0.05	2.27
				0.10	2.50
				0.20	7.69
1 M NaClO ₄ /PC	0.34	0.39	0.05	0.02	1.05
				0.05	1.05
				0.10	0.68
				0.20	0.41

The decrease in the current density associated with Na plating/stripping (increase in plating-stripping resistance) is likely related to the formation of a specific SEI on the sodium surface when it is in contact with an electrolyte containing SO_2 . Some authors have described such a process by means of Equations (2)–(5) [14,19]. Similar reactions have been proposed for a system based on Li-SO_2 [20,21].



Equation (5) is the simplest one that more straightforwardly accounts for the formation of an SEI in which the transport of sodium ions is expected to be efficient based on the low melting points reported for $\text{Na}_2\text{S}_2\text{O}_4$. However, the contribution of the other reactions cannot be discarded. XPS and in-situ Raman spectroscopy measurements are underway to clarify this question.

Examination of Figure 1 and Table 1 shows that, as the mole fraction of sulfur dioxide grows, there is a significant increase in the plating-stripping resistance, except in the case of the 1 M NaClO_4/PC electrolyte for which R_{ps} decreases as the SO_2 mole fraction increases.

In this particular case, for an SO_2 mole fraction of 0.20, the current density increases notably, becoming similar to that obtained in the absence of additive, but with a much higher stability as the plating-stripping resistance does not significantly change upon repeated cycling. Likely, the enhanced growth of the SEI in the presence of increasing amounts of SO_2 plays a role in the performance and kinetics of the Na^+/Na process, slowing it down and making it more robust. In contrast, a synergetic effect seems to happen in the NaClO_4 -based electrolyte, for which the current density increases as the concentration of additive does.

As observed in Table 1, the highest values for the resistance were obtained for relatively high contents of SO_2 in 1.6 M $\text{NaTf}/\text{DOL}:\text{DME}$. This is likely related to a drastic change in the electrolyte's nature, which becomes a gel. Actually, the solution was diluted by 20% with respect to that employed in the absence of SO_2 as to facilitate the measurements, and a SO_2 mole fraction of 0.2 was not studied because the electrolyte was fully gelled.

On the other hand, the development of anode-free batteries may represent important practical advantages as it may allow mounting SMBs in a fully discharged state, thus avoiding the handling of sodium metal. In this respect, sodium plating/stripping was also performed on a copper foil substrate. As with the sodium metal electrodes, CVs were acquired in both the presence and the absence of SO_2 . Figure 2 shows the corresponding CVs in the case of the $\text{NaTf}/\text{DOL}:\text{DME}$ electrolyte. Without additive, the electrolyte concentration was 2 M, while with SO_2 it was slightly lowered to 1.6 M (as explained previously). As observed in the red curve of Figure 2a, in the absence of SO_2 , there are no clear signs of sodium deposition on Cu, even reaching a potential as low as -0.2 V vs. Na^+/Na . However, low mole fractions of SO_2 favor the plating process, which occurs now at a low overvoltage and with significant reversibility. The Coulombic efficiency attains a value of 70% after adding a 0.02 SO_2 mole fraction.

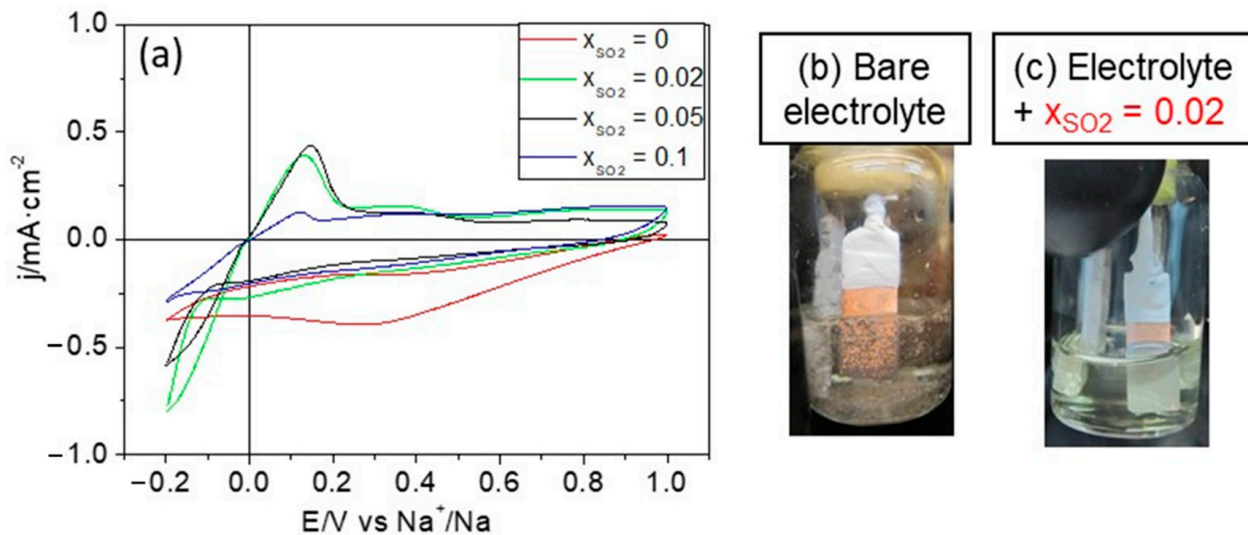


Figure 2. (a) CVs for the deposition of Na on Cu in 2 M or 1.6 M (in the presence of SO_2) $\text{NaTf}/\text{DOL}:\text{DME}$ at $20 \text{ mV}\cdot\text{s}^{-1}$ for different mole fractions of SO_2 . Pictures showing the sodium deposit morphology on Cu before (b) and after (c) adding a SO_2 mole fraction of 0.02. Pictures (b,c) were obtained after applying a potential of -0.2 V vs. Na^+/Na for 500 s.

The pictures in Figure 2b,c show the aspect of the sodium deposits on the Cu substrate obtained after applying a potential of -0.2 V vs. Na^+/Na for 500 s in the absence of and in the presence of the additive, respectively. It should be emphasized that the morphology of the sodium deposit dramatically changes upon the introduction of the additive, from one formed by particles that easily detach from the substrate to a continuous and homogeneous sodium deposit on the entire Cu surface in contact with the electrolyte. It is worth mentioning that this type of experimental result is not commonly reported in battery

research, and it is novel in the context of sodium batteries. We would like to emphasize that providing evidence on the quality and uniformity of the sodium deposit on a macroscopic level is very important from practical and technical points of view.

Equivalent experiments have been carried out for the electrolytes 2 M NaSCN/DOL:DME and 1 M NaClO₄/PC under the same conditions (scan rate of 20 mV s⁻¹ and negative potential limit of -0.2 V). Figure 3a shows the CVs for the Na plating/stripping process on Cu in 2 M NaSCN/DOL:DME without SO₂ and for various mole fractions thereof. The electrochemical plating of Na is clearly enhanced, even for low mole fractions of SO₂ as the additive significantly improves the Coulombic efficiency for the Na⁺/Na process as well as the associated currents. It is remarkable, though, that, for SO₂ mole fractions above 0.05, the enhancement is less substantial. In any case, the additive again favors that sodium can be homogeneously deposited on the copper surface, as demonstrated through a comparison of the electrode photographs in Figure 3b,c. They were obtained after applying to the copper electrode a potential of -0.2 V vs. Na⁺/Na for 500 s.

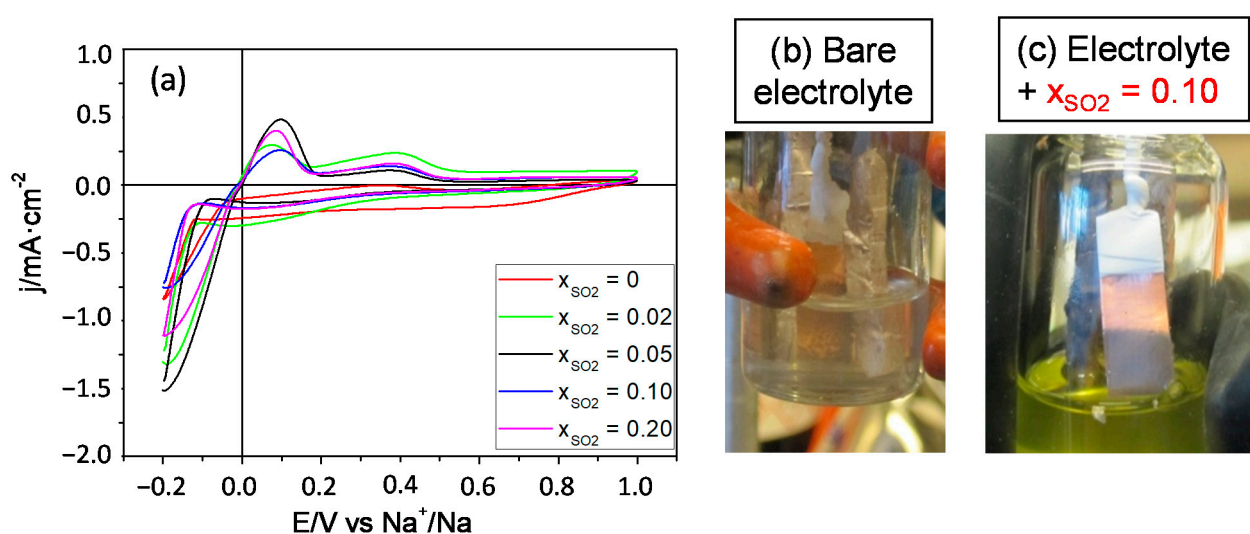


Figure 3. (a) CVs for the deposition of Na on Cu in 2 M NaSCN/DOL:DME at 20 mV s⁻¹ for different mole fractions of SO₂. Pictures (b,c) show the sodium deposit morphology on Cu before (b) and after (c) adding an SO₂ mole fraction of 0.10. They were taken after applying a potential of -0.2 V vs. Na⁺/Na for 500 s.

Figure 4 shows the plating/stripping process for Na on Cu in 1 M NaClO₄/PC. In this case, and as expected, the Na⁺/Na process shows partial reversibility even in the absence of SO₂. Interestingly, the current density increases with the concentration of the additive, contrary to what happened in the previous cases. Specifically, deposition currents more than double when SO₂ is present at a mole fraction of 0.20. This behavior is parallel to that shown by the sodium metal electrodes (see Figure 1). The use of other metal substrates (aluminum in particular) is underway in our laboratories.

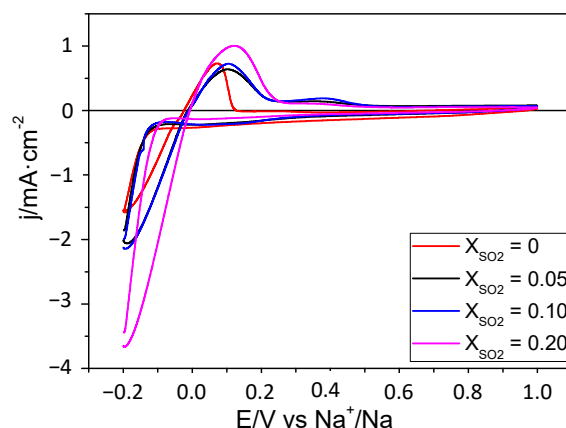


Figure 4. CVs for the deposition of Na on Cu in 1 M NaClO₄/PC at 20 mV s^{−1} for several SO₂ concentrations.

A study of the stability of the Na deposit on Cu was also carried out in 1 M NaClO₄/PC. In this case, Na was electrodeposited on Cu by applying a constant potential of -0.2 V for 500 s. Subsequently, several CVs were acquired at 20 mV s^{−1} using the potential limits of ± 0.2 V. Figure 5 shows the results obtained with and without additive. There is a certain decrease in the current density with the number of cycles, except when the SO₂ mole fraction is 0.20. In such a case, there is hardly any variation in the current after 20 cycles. It is also relevant that, in this case, the addition of SO₂ does not have a deleterious effect on the magnitude of the currents. In fact, attaining a mole fraction of 0.2 leads to a drop in the plating-stripping resistance, which halves the value in the absence of the additive. It is also relevant that the deposition of fresh sodium metal, which should entail the formation of a fresh SEI, also favors the reversibility of the Na plating/stripping process. This can be concluded from a comparison of the current densities in Figures 1 and 5 under the same polarization and it is also probably related to the existence of a certain roughness factor in the sodium metal deposit.

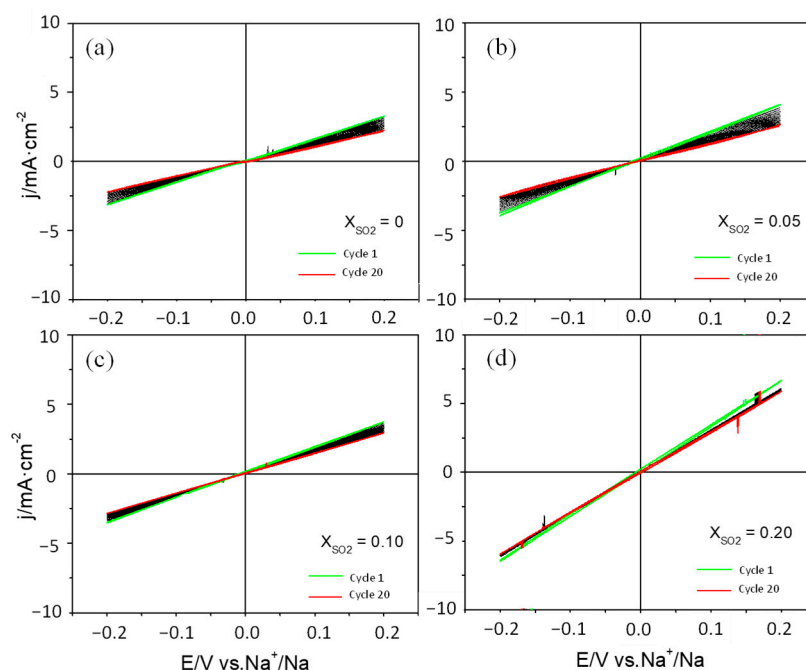


Figure 5. CVs for the Na⁺/Na process (on Cu) at 20 mV s^{−1} for mole fractions of SO₂: (a) 0; (b) 0.05; (c) 0.10; and (d) 0.20 in 1 M NaClO₄/PC. A thin film of Na was previously deposited in an additive-free electrolyte by applying a potential of -0.2 V for 500 s.

The use of SO₂ as an additive significantly reduces risks when compared to the use of SO₂ as a solvent. However, questions regarding a relatively high SO₂ partial pressure in equilibrium with the solution derived from the fact that SO₂ is a gas under normal conditions have motivated us to research on a closely related alternative. Specifically, we have considered the use of sulfolane as an additive, aiming again to enhance the Na plating/stripping process. Sulfolane is a dipolar aprotic solvent with a melting point of 27.5 °C, density of 1.261 g·cm⁻³, and viscosity of 0.01007 Pa·s at 30 °C. It is very stable; even at temperatures as high as 200 °C, the rate of decomposition is 0.009%/h [22]. In addition, sulfolane has been employed in the context of rechargeable Li-ion batteries, being used both as a solvent and as an additive in the electrolyte [23–25]. Sulfolane molecules can adsorb on the working electrode modifying the electrode–solution interface. Xing et al., through molecular simulation studies for solutions consisting of sulfolane, dimethyl carbonate and LiPF₆, reported that the oxygen atoms of the sulfolane molecule were strongly adsorbed on the substrate, while the carbonyl groups (coming from the solvent) were repelled when potential reaches sufficiently negative values, as is the case for sodium plating/stripping [26]. In addition, the behavior of the electrolyte was also reported to be a result of the strong interaction of sulfolane with the sodium cations. Another characteristic of sulfolane is its high electrochemical stability, reaching potentials above 5.8 V without decomposing [27–29]. However, sulfolane-based electrolytes show high viscosity, and, as a result, the wettability of the cathode is strongly affected. This is also a limitation for the transport of Na⁺ ions, particularly relevant for fast battery charging/discharging [24,28]. To minimize these deleterious effects, the use of sulfolane as an additive in Li electrolytes has been described. Cai et al. found that 2% sulfolane in the electrolyte increased, for a LiNi_{1/3}Co_{1/3}Mn_{1/3}O₂/graphite lithium-ion cell, the capacity of the initial discharge and the capacity retention, which changed from 53% to 63% after 100 cycles [30].

As far as we know, the use of sulfolane as an additive has not been described for Na-based batteries. Several mole fractions of sulfolane have been added to 1 M NaClO₄/PC and the Na plating/stripping process has been studied on a copper substrate in a three-electrode cell. Figure 6 shows ten successive cycles for the Na⁺/Na process in contact with electrolytes containing mole fractions of sulfolane ranging from 0.02 to 0.10. As observed in Figure 6a, in the absence of sulfolane, Na can be deposited on Cu, but the Coulombic efficiency of the process is below 80% ($Q_- > Q_+$). However, when a 0.02 mole fraction of sulfolane is added to the organic electrolyte, the voltammetric behavior undergoes a significant change. During the first cycles the reversibility of the process is very poor, and it shows low Coulombic efficiency. However, as the number of cycles increases, the current densities also increase, achieving a quasi-stationary behavior in the last three cycles, as shown in Figure 6b. It is worth noting that the attained current densities are higher (almost twofold) for a sulfolane mole fraction of 0.02. However, if the concentration of sulfolane is increased up to a mole fraction of 0.10, the shape of the voltammogram changes drastically and the Na⁺/Na process is barely discernible. This is likely related to a partial gelation of the electrolyte. When the sulfolane mole fraction reaches a value of 0.20, the electrolyte is fully gelled (see a picture of the electrolyte in an inverted vial in Figure 6d) and no electrochemical experiments were carried out.

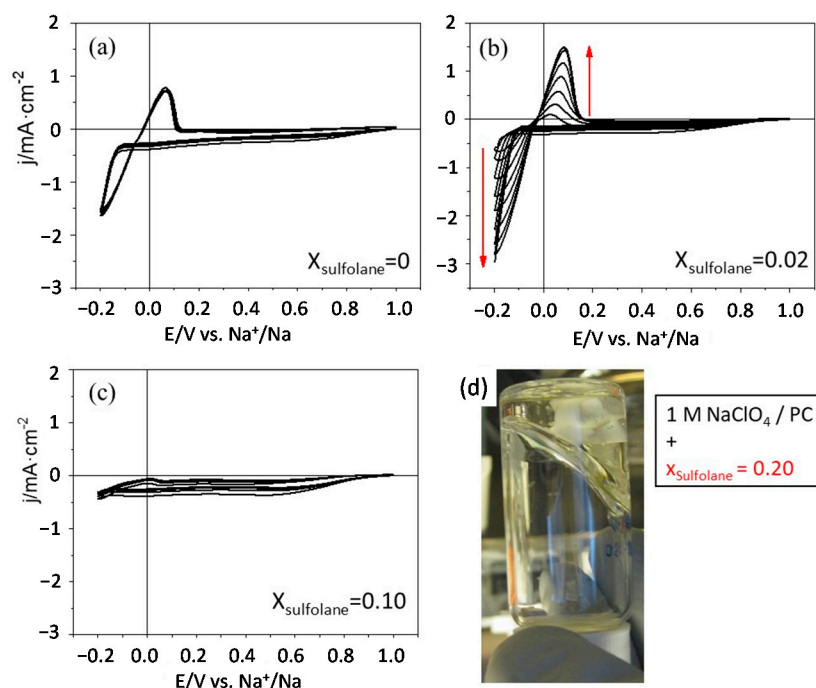


Figure 6. CVs at 20 mVs^{-1} for the plating/stripping of Na on Cu in $1 \text{ M NaClO}_4/\text{PC}$ with different mole fractions of sulfolane: (a) 0; (b) 0.02 and (c) 0.10. (d) Picture showing the aspect of a $1 \text{ M NaClO}_4/\text{PC}$ solution with a 0.20 mole fraction of sulfolane.

The improvement induced in the Na deposition process by the presence of sulfolane is related to the adsorption of the additive molecules on both copper and sodium, which is likely followed by their spontaneous reduction. Such an adsorption is probably favored at negative potentials because of the expected strong interaction of the additive molecules with the sodium ions. According to the literature, SO_2 is adsorbed perpendicularly to the surface of Cu and the interaction between adsorbate and adsorbent can occur either through the S atom, or through the S atom and at least one of the O atoms (Figure 7a) [21–34]. The formation of this adlayer should further favor both the approach of the Na^+ ions to the metal surface and their reduction, facilitating the Na^+/Na plating process [35–38].

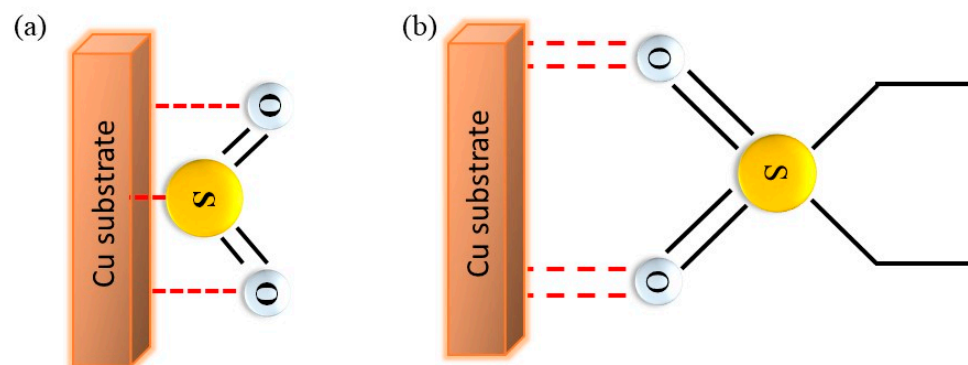
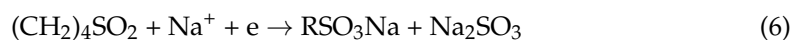


Figure 7. (a) Schematic representations for the interaction of (a) SO_2 and (b) sulfolane with the Cu substrate.

The results shown in Figure 6 for the $1 \text{ M NaClO}_4/\text{PC}$ electrolyte with sulfolane as an additive suggest a modification of the electrode-solution interface due to the adsorption of the sulfolane molecules on Cu (Figure 7b), which improves the Na^+/Na process. Furthermore, sulfolane can also be involved in the formation of a stable SEI on the working

electrode. By analogy with the behavior described for a Li-ion battery, the following unbalanced equation would be proposed [39]:



The progressive formation of an SEI according to Equation (6) would explain the evolution of the voltammetric current density with the number of cycles observed in Figure 6b. In situ and ex situ characterization with Raman spectroscopy and XPS, respectively, are also underway in our laboratory to shed light on this question.

3. Materials and Methods

3.1. Synthesis of Organic Electrolytes

NaCF_3SO_3 (NaTf, 98% TCI, Tokyo, Japan), NaSCN ($\geq 98\%$, Fluka, CERN, Meyrin, Switzerland), NaClO_4 (98%, Sigma Aldrich, Burlington, MA, USA) were dried at 100°C in a vacuum oven overnight prior to use. Dimethoxyethane (DME), 1,4-dioxolane (DOL), and propylene carbonate (PC) were 99.8% anhydrous (Sigma Aldrich, Burlington, MA, USA) and were used as received. The organic electrolyte was prepared by dissolving the corresponding amount of sodium salt in the corresponding organic solvent. SO_2 (99%, Air Liquide, Paris, France) was condensed at -18°C and the required amount of additive was added as a liquid to the organic electrolyte. Sulfolane (99%, Sigma Aldrich, Burlington, MA, USA) was added as received to the organic electrolyte. After adding either SO_2 or sulfolane, the electrolytes were stirred 30 min prior to characterization.

3.2. Electrochemical Measurements

Electrochemical tests were performed by means of a three-electrode electrochemical cell in which sodium metal pieces were used as reference and counter electrodes (sodium rods with dimensions $0.5 \times 0.5 \times 1$ cm), while either copper foil or a sodium rod was used as a working electrode. The geometric area of the working electrode in contact with the electrolyte was of 1 cm^2 . The cells were assembled in a nitrogen-filled glovebox with a concentration of moisture and oxygen below 0.5 ppm. All the electrochemical experiments were run at room temperature, and a scan rate of $20\text{ mV}\cdot\text{s}^{-1}$ was used for recording the CVs. An Orignalys potentiostat-galvanostat (OGF-500) was used to carry out electrochemical experiments.

4. Conclusions

This work describes for the first time the use of SO_2 -based compounds as additives in organic electrolytes to enhance the sodium plating/stripping process. Relatively low mole fractions of SO_2 in electrolytes such as NaTf/DOL:DME, NaSCN/DOL:DME and NaClO_4 /PC stabilize the Na^+/Na process as revealed by the smaller changes experienced by the current-potential curves in the presence of the additive upon repeated voltammetric cycling. When bare copper is used as a substrate, the Coulombic efficiency for the Na plating/stripping process significantly improves in the presence of SO_2 . This is particularly relevant from a practical perspective as it means that it would be possible to assemble a battery with an anode-free configuration, avoiding the handling of sodium metal. Furthermore, an increase in the current density for sodium plating/stripping has also been observed when copper substrates with freshly deposited thin films of sodium were used, which indicates an enhancement of the electrolyte and interphasial properties in the presence of the additive. Similar results were obtained in the case of sulfolane as an additive in the NaClO_4 /PC electrolyte. Not only was an increase in the Coulombic efficiency observed when copper was used as a substrate, but also larger current densities were achieved for the same overpotentials (lower plating-stripping resistances) in comparison with the additive-free electrolyte. However, a larger amount of any of these additives in the electrolytes may lead to gel formation, thus seriously impacting on their viscosity and the efficiency of the electrochemical processes.

The improvement observed in most cases in the presence of the SO₂-based additives is attributed to both the favorable interaction of the additive molecules with the sodium ions and the specific adsorption of the sulfur-containing molecule on the metal surface, which promote sodium deposition. In addition, the formation of an SEI on the sodium surface should be considered. In the case of SO₂ as an additive, Na₂S₂O₄ (Equation (5)) is expected to be the main component of the SEI, while RSO₃Na and Na₂SO₃ would be present when sulfolane is added (Equation (6)). Further investigation is underway to confirm some of these hypotheses.

Finally, it is remarkable that both sulfur-based additives could be employed in the formulation of new organic electrolytes for sodium metal batteries, using either a sodium metal anode or an anode-free configuration. The additive mole fractions needed are relatively low, thus avoiding the main drawbacks of these compounds when used as solvents: corrosivity and high volatility (in the case of SO₂) and high viscosity (in the case of sulfolane). From a practical perspective, it should also be considered that sulfolane can be handled more easily than SO₂, which is a gas under normal conditions. In addition, the partial pressure of the additive in equilibrium with the electrolyte is much lower for sulfolane, favoring the stability of the solution under a wider range of conditions (relatively high temperatures).

Supplementary Materials: The following supporting information can be downloaded at: <https://www.mdpi.com/article/10.3390/batteries8090127/s1>, Figure S1: CVs for Na-on-Na deposition/stripping in: (a,b) 2M NaTf /DOL:DME without and with 0.02 SO₂ mole fraction. (c,d) 1.6 M NaTf /DOL:DME with 0.05 and 0.1 SO₂ mole fraction; Figure S2: CVs for Na-on-Na deposition/stripping in 2 M NaSCN/DOL:DME containing SO₂ mole fractions of (a) 0, (b) 0.02, (c) 0.05, (d) 0.10 and (e) 0.20; Figure S3. Cyclic voltammograms for Na-on-Na deposition/stripping in 1 M NaClO₄/PC containing SO₂ mole fractions of (a) 0, (b) 0.05, (c) 0.10 and (d) 0.20.

Author Contributions: Conceptualization, D.R.-M. and R.G.; Methodology, D.R.-M. and R.G.; Validation, D.R.-M. and R.G.; Formal Analysis, R.G.; Investigation, D.R.-M.; Resources, R.G.; Data Curation, D.R.-M.; Writing—Original Draft Preparation, D.R.-M.; Writing—Review & Editing, D.R.-M. and R.G.; Visualization, D.R.-M.; Supervision, D.R.-M. and R.G.; Project Administration, R.G.; Funding Acquisition, R.G. All authors have read and agreed to the published version of the manuscript.

Funding: This research was partially funded by the Ministerio de Ciencia e Innovación/Agencia Estatal de Investigación/Fondos FEDER through project RTI2018-102061-B-I00 and by the Generalitat Valenciana through project PROMETEO/2020/089.

Institutional Review Board Statement: Not applicable.

Informed Consent Statement: Not applicable.

Data Availability Statement: The data presented in this study are available in the article.

Acknowledgments: We are grateful to Andras Kovacs from BROADBIT for fruitful discussions and to the funding agencies supporting our work.

Conflicts of Interest: The authors declare no conflict of interest.

References

1. Coetzer, J. A New High Energy Density Battery System. *J. Power Sources* **1986**, *18*, 377–380. [[CrossRef](#)]
2. Dustmann, C.-H. Advances in ZEBRA Batteries. *J. Power Sources* **2004**, *127*, 85–92. [[CrossRef](#)]
3. Kim, B.-R.; Jeong, G.; Kim, A.; Kim, Y.; Kim, M.G.; Kim, H.; Kim, Y.-J. High Performance Na-CuCl₂ Rechargeable Battery toward Room Temperature ZEBRA-Type Battery. *Adv. Energy Mater.* **2016**, *6*, 1600862. [[CrossRef](#)]
4. Zheng, X.; Bommier, C.; Luo, W.; Jiang, L.; Hao, Y.; Huang, Y. Sodium Metal Anodes for Room-Temperature Sodium-Ion Batteries: Applications, Challenges and Solutions. *Energy Storage Mater.* **2019**, *16*, 6–23. [[CrossRef](#)]
5. Lee, J.; Kim, J.; Kim, S.; Jo, C.; Lee, J. A Review on Recent Approaches for Designing the SEI Layer on Sodium Metal Anodes. *Mater. Adv.* **2020**, *1*, 3143–3166. [[CrossRef](#)]
6. Liu, W.; Liu, P.; Mitlin, D. Review of Emerging Concepts in SEI Analysis and Artificial SEI Membranes for Lithium, Sodium, and Potassium Metal Battery Anodes. *Adv. Energy Mater.* **2020**, *10*, 2002297. [[CrossRef](#)]

7. Gao, L.; Chen, J.; Chen, Q.; Kong, X. The Chemical Evolution of Solid Electrolyte Interface in Sodium Metal Batteries. *Sci. Adv.* **2022**, *8*, eabm4606. [[CrossRef](#)]
8. Giffin, G.A. Ionic Liquid-Based Electrolytes for “Beyond Lithium” Battery Technologies. *J. Mater. Chem. A* **2016**, *4*, 13378–13389. [[CrossRef](#)]
9. Hilder, M.; Howlett, P.; Saurel, D.; Gonzalo, E.; Basile, A.; Armand, M.; Rojo, T.; Kar, M.; MacFarlane, D.R.; Forsyth, M. The Effect of Cation Chemistry on Physicochemical Behaviour of Superconcentrated NaFSI Based Ionic Liquid Electrolytes and the Implications for Na Battery Performance. *Electrochim. Acta* **2018**, *268*, 94–100. [[CrossRef](#)]
10. Monti, D.; Ponrouch, A.; Palacín, M.R.; Johansson, P. Towards Safer Sodium-Ion Batteries via Organic Solvent/Ionic Liquid Based Hybrid Electrolytes. *J. Power Sources* **2016**, *324*, 712–721. [[CrossRef](#)]
11. Vélez, J.F.; Álvarez, L.V.; del Río, C.; Herradón, B.; Mann, E.; Morales, E. Imidazolium-Based Mono and Dicationic Ionic Liquid Sodium Polymer Gel Electrolytes. *Electrochim. Acta* **2017**, *241*, 517–525. [[CrossRef](#)]
12. Brissot, C.; Rosso, M.; Chazalviel, J.-N.; Lascaud, S. Dendritic Growth Mechanisms in Lithium/Polymer Cells. *J. Power Sources* **1999**, *81–82*, 925–929. [[CrossRef](#)]
13. Cao, R.; Mishra, K.; Li, X.; Qian, J.; Engelhard, M.H.; Bowden, M.E.; Han, K.S.; Mueller, K.T.; Henderson, W.A.; Zhang, J.G. Enabling Room Temperature Sodium Metal Batteries. *Nano Energy* **2016**, *30*, 825–830. [[CrossRef](#)]
14. Jeong, G.; Kim, H.; Sug Lee, H.; Han, Y.K.; Hwan Park, J.; Hwan Jeon, J.; Song, J.; Lee, K.; Yim, T.; Jae Kim, K.; et al. A Room Temperature Sodium Rechargeable Battery Using an SO₂-Based Nonflammable Inorganic Liquid Catholyte. *Sci. Rep.* **2015**, *5*, 12827. [[CrossRef](#)]
15. Song, J.; Jeong, G.; Lee, A.J.; Park, J.H.; Kim, H.; Kim, Y.J. Dendrite-Free Polygonal Sodium Deposition with Excellent Interfacial Stability in a NaAlCl₄-2SO₂ Inorganic Electrolyte. *ACS Appl. Mater. Interfaces* **2015**, *7*, 27206–27214. [[CrossRef](#)] [[PubMed](#)]
16. Ruiz-Martínez, D.; Kovacs, A.; Gómez, R. Development of Novel Inorganic Electrolytes for Room Temperature Rechargeable Sodium Metal Batteries. *Energy Environ. Sci.* **2017**, *10*, 1936–1941. [[CrossRef](#)]
17. Wang, Z.; Lu, K.; Xia, F.; Dahunsi, O.; Gao, S.; Li, B.; Wang, R.; Lu, D.; Qin, W.; Cheng, Y.; et al. Sodiated Na_xSnSb nanoparticles embedded in N-doped graphene sponges direct uniform Na nucleation and smooth plating for high efficiency Na metal batteries. *J. Mater. Chem. A* **2021**, *9*, 6123–6130. [[CrossRef](#)]
18. Genovese, M.; Louli, A.J.; Weber, R.; Sanderson, R.J.; Johnson, M.B.; Dahn, J.R. Combinatorial Methods for Improving Lithium Metal Cycling Efficiency. *J. Electrochem. Soc.* **2018**, *165*, A3000–A3013. [[CrossRef](#)]
19. Chastain, J.; King, R.C. *Handbook of X-ray Photoelectron Spectroscopy: A Reference Book of Standard Spectra for Identification and Interpretation of XPS Data*; Perkin-Elmer: Eden Prairie, MN, USA, 1992.
20. Dey, A.N.; Kuo, H.C.; Piliero, P.; Kallianidis, M. Inorganic Electrolyte Li/SO₂ Rechargeable System Development of a Prototype Hermetic C Cell and Evaluation of Its Performance and Safety Characteristics. *J. Electrochem. Soc.* **1988**, *135*, 2115–2120. [[CrossRef](#)]
21. Dey, A.N. Inorganic Electrolyte Li/CuCl₂ Rechargeable Cell. *J. Electrochem. Soc.* **1989**, *136*, 1618–1621. [[CrossRef](#)]
22. Tilstam, U. Sulfolane: A Versatile Dipolar Aprotic Solvent. *Org. Process Res. Dev.* **2012**, *16*, 1273–1278. [[CrossRef](#)]
23. Lewandowski, A.; Kurc, B.; Stepniak, I.; Swiderska-Mocek, A. Properties of Li-Graphite and LiFePO₄ Electrodes in LiPF₆-Sulfolane Electrolyte. *Electrochim. Acta* **2011**, *56*, 5972–5978. [[CrossRef](#)]
24. Li, S.; Li, B.; Xu, X.; Shi, X.; Zhao, Y.; Mao, L.; Cui, X. Electrochemical Performances of Two Kinds of Electrolytes Based on Lithium Bis(Oxalate)Borate and Sulfolane for Advanced Lithium Ion Batteries. *J. Power Sources* **2012**, *209*, 295–300. [[CrossRef](#)]
25. Hirata, K.; Morita, Y.; Kawase, T.; Sumida, Y. Electrochemical Performance of an Ethylene Carbonate-Free Electrolyte Based on Lithium Bis(Fluorosulfonyl)Imide and Sulfolane. *J. Power Sources* **2018**, *395*, 163–173. [[CrossRef](#)]
26. Xing, L.; Vatamanu, J.; Borodin, O.; Smith, G.D.; Bedrov, D. Electrode/Electrolyte Interface in Sulfolane-Based Electrolytes for Li Ion Batteries: A Molecular Dynamics Simulation Study. *J. Phys. Chem. C* **2012**, *116*, 23871–23881. [[CrossRef](#)]
27. Sun, X.G.; Angell, C.A. New Sulfone Electrolytes for Rechargeable Lithium Batteries. Part I. Oligoether-Containing Sulfones. *Electrochem. Commun.* **2005**, *7*, 261–266. [[CrossRef](#)]
28. Xu, K.; Angell, C.A. Sulfone-Based Electrolytes for Li-Ion Batteries. *J. Electrochem. Soc.* **2002**, *149*, A920–A926. [[CrossRef](#)]
29. Watanabe, Y.; Kinoshita, S.-i.; Wada, S.; Hoshino, K.; Morimoto, H.; Tobishima, S.-i. Electrochemical Properties and Lithium Ion Solvation Behavior of Sulfone-Ester Mixed Electrolytes for High-Voltage Rechargeable Lithium Cells. *J. Power Sources* **2008**, *179*, 770–779. [[CrossRef](#)]
30. Cai, H.; Jing, H.; Zhang, X.; Shen, M.; Wang, Q. Improving High-Voltage Performance of Lithium-Ion Batteries with Sulfolane as an Electrolyte Additive. *J. Electrochem. Soc.* **2017**, *164*, A714–A720. [[CrossRef](#)]
31. Baxter, J.P.; Grunze, M.; Kong, C.W. Interaction of SO₂ with Copper and Copper Oxide Surfaces. *J. Vac. Sci. Technol. A Vac. Surfaces Films.* **1988**, *6*, 1123–1127. [[CrossRef](#)]
32. Galtayries, A.; Grimblot, J.; Bonnelle, J.-P. Interaction of SO₂ with Different Polycrystalline Cu, Cu₂O and CuO Surfaces. *Surf. Interface Anal.* **1996**, *24*, 345–354. [[CrossRef](#)]
33. Nakahashi, T.; Terada, S.; Yokoyama, T.; Hamamatsu, H.; Kitajima, Y.; Sakano, M.; Matsui, F.; Ohta, T. Adsorption of SO₂ on Cu(100) Studied by X-ray Absorption Fine Structure Spectroscopy and Scanning Tunneling Microscopy. *Surf. Sci.* **1997**, *373*, 1–10. [[CrossRef](#)]
34. Pangher, N.; Wilde, L.; Polcik, M.; Haase, J. Structure Determinations of SO₂ and Its Decomposition Product SO Adsorbed on Cu(100) by Use of X-ray Absorption Fine-Structure Measurements. *Surf. Sci.* **1997**, *372*, 211–222. [[CrossRef](#)]

35. Monteiro, M.J.; Ando, R.A.; Siqueira, L.J.A.; Camilo, F.F.; Santos, P.S.; Ribeiro, M.C.C.; Torresi, R.M. Effect of SO₂ on the Transport Properties of an Imidazolium Ionic Liquid and Its Lithium Solution. *J. Phys. Chem. B* **2011**, *115*, 9662–9670. [[CrossRef](#)] [[PubMed](#)]
36. Ein-Eli, Y.; Thomas, S.R.; Koch, V.R. The Role of SO₂ as an Additive to Organic Li-Ion Battery Electrolytes. *J. Electrochem. Soc.* **1997**, *144*, 1159–1165. [[CrossRef](#)]
37. Abraham, K.M.; Chaudhri, S.M. The Lithium Surface Film in the Li/SO₂ Cell. *J. Electrochem. Soc.* **1986**, *133*, 1307–1311. [[CrossRef](#)]
38. Ein-Eli, Y.; Thomas, S.R.; Koch, V.R. New Electrolyte System for Li-Ion Battery. *J. Electrochem. Soc.* **1996**, *143*, L195–L197. [[CrossRef](#)]
39. Li, S.; Xu, X.; Shi, X.; Li, B.; Zhao, Y.; Zhang, H.; Li, Y.; Zhao, W.; Cui, X.; Mao, L. Composition Analysis of the Solid Electrolyte Interphase Film on Carbon Electrode of Lithium-Ion Battery Based on Lithium Difluoro(Oxalate)Borate and Sulfolane. *J. Power Sources* **2012**, *217*, 503–508. [[CrossRef](#)]